EDGE ARTICLE

Check for updates

The ubiquitous cross-coupling catalyst system 'Pd(OAc)₂'/2PPh₃ forms a unique dinuclear PdI complex: an important entry point into catalytically competent cyclic Pd₃ clusters†

Neil W. J. Scott, [ID] [a] Mark J. Ford, [b] Christoph Schotes, [c] Rachel R. Parker, [ID] [a] Adrian C. Whitwood [ID] [a] and Ian J. S. Fairlamb [ID] *[a]

Palladium(II) acetate 'Pd(OAc)₂'/nPPh₃ is a ubiquitous precatalyst system for cross-coupling reactions. It is widely accepted that reduction of *in situ* generated *trans*-[Pd(OAc)₂(PPh₃)₂] affords [Pd⁰(PPh₃)ₙ] and/or [Pd⁰(PPh₃)₂(OAc)]⁻ species which undergo oxidative addition reactions with organohalides – the first committed step in cross-coupling catalytic cycles. In this paper we report for the first time that reaction of Pd₃(OAc)₆ with 6 equivalents of PPh₃ (*i.e.* a Pd/PPh₃ ratio of 1 : 2) affords a novel dinuclear PdI complex [Pd₂(μ-PPh₂)(μ₂-OAc)(PPh₃)₂] as the major product, the elusive species resisting characterization until now. While unstable, the dinuclear PdI complex reacts with CH₂Cl₂, *p*-fluoroiodobenzene or 2-bromopyridine to afford Pd₃ cluster complexes containing bridging halide ligands, *i.e.* [Pd₃(X)(PPh₂)₂(PPh₃)₃]X, carrying an overall 4/3 oxidation state (at Pd). Use of 2-bromopyridine was critical in understanding that a putative 14-electron mononuclear 'PdII(R)(X)(PPh₃)' is released on forming [Pd₃(X)(PPh₂)₂(PPh₃)₃]X clusters from [Pd₂(μ-PPh₂)(μ₂-OAc)(PPh₃)₂]. Altering the Pd/PPh₃ ratio to 1 : 4 forms Pd⁰(PPh₃)₃ quantitatively. In an exemplar Suzuki–Miyaura cross-coupling reaction, the importance of the 'Pd(OAc)₂'/nPPh₃ ratio is demonstrated; catalytic efficacy is significantly enhanced when *n* = 2. Employing 'Pd(OAc)₂'/PPh₃ in a 1 : 2 ratio leads to the generation of [Pd₂(μ-PPh₂)(μ₂-OAc)(PPh₃)₂] which upon reaction with organohalides (*i.e.* substrate) forms a reactive Pd₃ cluster species. These higher nuclearity species are the cross-coupling catalyst species, when employing a 'Pd(OAc)₂'/PPh₃ of 1 : 2, for which there are profound implications for understanding downstream product selectivities and chemo-, regio- and stereoselectivities, particularly when employing PPh₃ as the ligand.

Introduction

Palladium(II) acetate 'Pd(OAc)₂' is commonly used in combination with tertiary phosphine ligands, *e.g.* PPh₃, to generate active catalyst species for an eclectic array of cross-coupling reactions,[1] where it is universally accepted that 'Pd⁰(PPh₃)ₙ' species are formed.[2] Such species enter into oxidative reactions with organohalides, *e.g.* iodobenzene to generate *trans*-[Pd(I)(Ph)(PPh₃)₂].[3] Considerable and notable efforts have been made by Amatore and Jutand[4] to understand how varying the 'Pd(OAc)₂'/nPPh₃

ratio affects the generation of reduced palladium species in both THF and DMF. Following extensive NMR spectroscopic and electrochemical measurements, conclusions were drawn implicating phosphine-induced reduction of 'Pd(OAc)₂'/nPPh₃ mixtures, *via* *trans*-[Pd(OAc)₂(PPh₃)₂], by an intramolecular process (independent of phosphine concentration, once the latter complex is formed).[4] The global findings from Amatore and Jutand are detailed in Scheme 1, showing the key intermediate species observed by ³¹P NMR spectroscopic studies. Comparisons of these data were made with complexes generated from [Pd(PPh₃)₄] in the presence of *n*-Bu₄NOAc,[4a] under electrochemical conditions. The conclusions were that 'Pd⁰(PPh₃)ₙ' species are generated *in situ* from the reaction of Pd(OAc)₂'/2PPh₃ mixtures.[4a] Later studies showed that increasing the Pd/PPh₃ ratio to 1 : 3 and above led to the clean generation of [Pd⁰(PPh₃)ₙ(OAc)]⁻ species (*n* = 2 or 3), with O=PPh₃ being a key side product, *i.e.* formed during the formal PdII → Pd⁰ reduction process.[4b,c] Both 'Pd⁰(PPh₃)₂' and [Pd⁰(PPh₃)₂(OAc)]⁻ species react by oxidative addition with organohalides.

[a]Department of Chemistry, University of York, Heslington, York, North Yorkshire, YO10 5DD, UK. E-mail: ian.fairlamb@york.ac.uk

[b]Bayer Aktiengesellschaft, Crop Science Division, Industriepark Höchst G836, 65926 Frankfurt am Main, Germany

[c]Bayer AG, Crop Science Division, Building A729, 415, 41539 Dormagen, Germany

† Electronic supplementary information (ESI) available: Full experimental details and characterization data for all compounds is provided, including NMR spectra, X-ray diffraction data and computational data (as a PDF file). CCDC 1894927–1894931 and 1901195. For ESI and crystallographic data in CIF or other electronic format see DOI: 10.1039/c9sc01847f
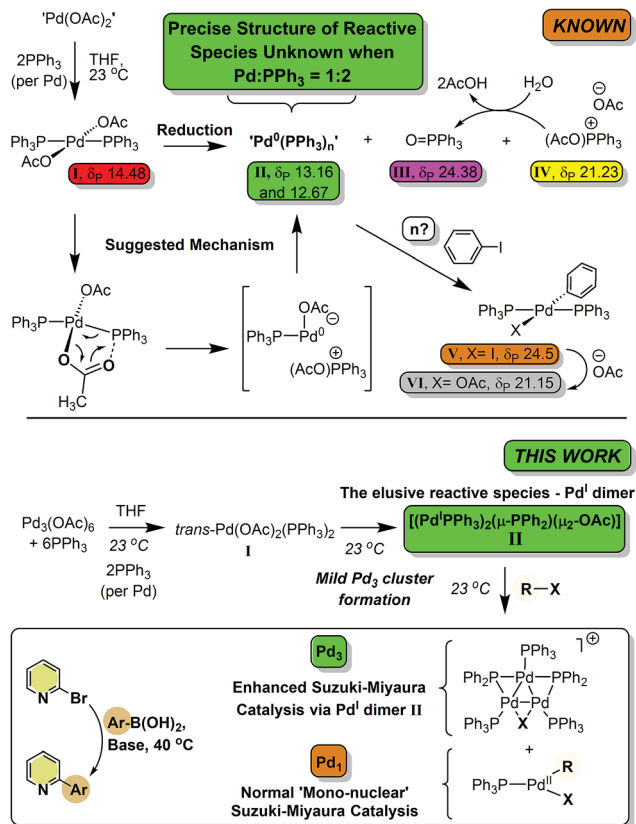
**Scheme 1** Reactions of 'Pd(OAc)₂' with PPh₃ (1 : 2 ratio). ³¹P NMR spectral data are taken from ref. 4a.

Later, Kollár et al. examined the reaction of 'Pd(OAc)₂'/nPPh₃ in DMF,[5] amongst other phosphines, concluding that 'Pd⁰(PPh₃)ₙ' species are formed under ambient reaction conditions. Taken together these studies suggest that a Pd/PPh₃ ratio of 1 : 3 is necessary for satisfactory catalytic cross-coupling performance.

Over the last 20 years we have regularly debated the differences in cross-coupling catalyst system performance on changing the Pd/PPh₃ ratio from 1 : 2 to 1 : 3.[6] When papers are reported employing a Pd/PPh₃ ratio of 1 : 2 we have asked the why, as 1 : 3 would be ideal based on the outcomes of previous studies;[4] in other words, optimal conditions for forming catalytically active [Pd⁰(PPh₃)ₙ(OAc)]⁻ species requires ≥3 equivalents of PPh₃ per Pd, "not 2 equivalents", when 'Pd(OAc)₂' is used as the initial Pd^II precatalyst.

A superb recent example is found in the high-throughput automated reaction screening study conducted by a team from Pfizer,[7] where a Pd/PPh₃ ratio of 1 : 2 was used for 480 Suzuki–Miyaura cross-coupling (SMCC) reactions, involving changes in solvent and base, against relatively minor changes in substrate structure, correlated alongside many other phosphine ligands (over 5760 reactions in total). Cronin et al. further applied a machine learning algorithm based on the product percentage yields.[8] With such important developments being made in automation, reaction optimization and machine learning,[9] knowing precisely the reactive Pd species,

formed under working reaction conditions, has never been more important. Thus, herein we report that the reaction of Pd₃(OAc)₆ with 6 equivalents of PPh₃ (Pd : PPh₃, 1 : 2) in both THF and DMF, generates a well-defined [Pd₂(μ-PPh₂)(μ₂-OAc)(PPh₃)₂] complex **II**. The formation of this unusual species adds to the mechanistic debate concerning the activation pathways for Pd(II) precatalysts, particularly papers reported by: (a) Balcells and Hazari[10a] showing formation of Pd^I dimers with NHC ligands and bridging allyl and chloride ligands (eqn (1)); (b) Colacot and Schoenebeck[10b] showing formation of Pd^I dimers with phosphines and bridging bromide ligands (eqn (2)); (c) Bedford[10c] showing SPhos activation on reaction with Pd(OAc)₂ (eqn (3)); (d) Jutand and Grimaud[10d] showing XPhos reactions with Pd(OAc)₂ leading to a proposed Pd^I dimer (eqn (4)).

The stability and reactivity of these Pd^I dimers appear to be critical in understanding the delivery of active 'L–Pd⁰' species, a process dependent on L/Pd ratios and additives. From our study we find that [Pd₂(μ-PPh₂)(μ₂-OAc)(PPh₃)₂] **II**, exhibits unique reactivity toward organohalides, e.g. CH₂Cl₂ **1a**, p-fluoro-iodobenzene **1b** and 2-bromopyridine **1c**, which affords Pd₃ cluster species, namely [Pd₃(X)(μ-PPh₂)₂(PPh₃)₃]X **VII** (later referred to as **Pd₃X·X**, where X = Cl, Br, I or OAc). Our results naturally connect to a recent report showing that **Pd₃Cl·Cl** is a highly active catalyst for SMCC reactions, including the activation of substrates containing harder to activate C–Cl bonds.[11] **Pd₃Cl·Cl** invokes an unusual switch in cross-coupling steps from oxidative addition then transmetallation to transmetallation and then oxidative addition.[11]
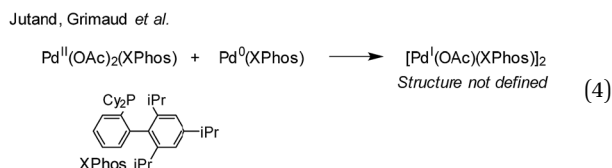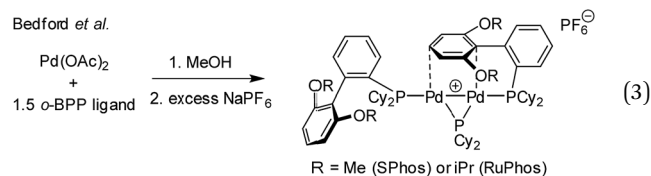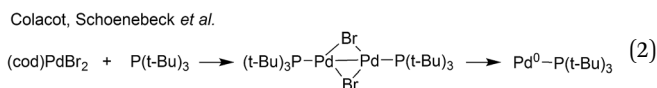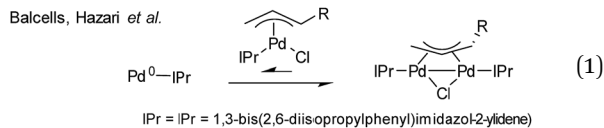
Results and discussion

The reaction of ultra-pure $Pd_3(OAc)_6$ (>99% purity) with PPh_3, in varying ratios, in THF-d_8 were conducted at room temperature (25 °C) and monitored by ^1H and ^{31}P NMR spectroscopic analysis (where [Pd] = 20 mM; T = 298 K, external reference = 85% H_3PO_4 in H_2O). A wide spectral window (−50 to +250 ppm) was required to allow full characterization of the array of phosphorus signals and associated species formed under these reaction conditions (Fig. 1 and 2).

Where the ratio of Pd : PPh_3 was 1 : 1, degradation of $Pd_3(OAc)_6$, leading to the formation of large perfectly spherical Pd particles (sized ∼0.1–0.4 μm, by TEM) and many P-containing species (by ^{31}P NMR) was observed (Fig. 1(a)). Alteration of the Pd/PPh_3 ratio to 1 : 2 (Fig. 1(b)) led to the

Fig. 1 The room temperature formation of dinuclear Pd(II) complexes from trans-$Pd(OAc)_2(PPh_3)_2$ in THF. (a) Ratio of Pd : PPh_3 = 1 : 1; (b) ratio of Pd : PPh_3 = 1 : 2; (c) ratio of Pd : PPh_3 = 1 : 3; (d) ratio of Pd : PPh_3 = 1 : 4. The Pd^0 species $Pd^0(PPh_3)_3$ **IX** and $[Pd^0(PPh_3)_3OAc]^−$ **IX'** are indicated by cyan circles (appearing as coincident signals by ^{31}P NMR spectroscopic analysis when present together – compare top two ^{31}P NMR spectra in Fig. 2 with the authentic sample of $Pd^0(PPh_3)_3$ **IX**, bottom spectrum, Fig. 2).

formation of a major new phosphorus-containing species at $δ$ 199.01 (t, 1P) and $δ$ 13.41 (d, 2P), with a $^2J_{PP}$ coupling constant of 83.5 Hz (i.e. an AX$_2$ type spin system). The high ^{31}P chemical shift of $δ$ 199.01 indicates that the PPh_3 ligand has been activated by P–C bond-cleavage to give a bridging phosphido-group at Pd, with concomitant loss of 'C_6H_5'. The ^1H NMR spectrum shows a methyl resonance at $δ$ 2.08 (s, 3H), due to a bridging acetoxy ligand, which balances with aromatic proton integrals (40H). Running the reaction at lower $Pd_3(OAc)_6$ concentration (between 3 and 20 mM) allowed this species to be isolated in a form that could be crystallized. X-ray diffraction analysis of dark red single crystals of this species confirmed its structure as $[Pd_2(μ-PPh_2)(μ_2-OAc)(PPh_3)_2]$ **II**, possessing both bridging $μ_2$-acetoxy and $μ$-phosphido ligands and terminal-capping PPh_3 ligands. Complex **II** is a diamagnetic species. The Pd–Pd bond distance was found to be 2.5958(3) Å, which is in-keeping with other dinuclear Pd^I complexes with bridging $μ$-acetoxy ligands known in the literature (typical Pd–Pd distances 2.532 to 2.711 Å), and shorter than a related structure, $[Pd_2(η^3-allyl)(μ-OC(O)i-Bu)(PPh_3)_2]$ where the Pd···Pd bond distance equals 2.6267(3).[12]

A scaled-up synthesis of **II** was found possible from $Pd_3(OAc)_6$/$6PPh_3$, formed in 31% yield (note: some Pd is lost as large particles during its preparation), which was fully characterized. Interestingly, the LIFDI-MS data showed that the dinuclear Pd^I complex was present in solution (M$^{+•}$ = m/z 982, with the correct isotopic distribution). The reference ^{31}P NMR spectrum for purified **II** is given in Fig. 2 (externally-referenced to H_3PO_4). GC-MS analysis of the crude reaction mixture containing **II** indicated that benzene and biphenyl were present, the former most likely derived from protonation of 'Pd–Ph' species by adventitious water/AcOH and the latter by reductive elimination. Acetoxybenzene, a possible reductive elimination product, was not detected by GC-MS analysis. These species are accompanied by O=PPh_3 **III**, $[Ph_3P(OAc)]X$ **IV** and another dinuclear Pd^{II} species **VIII**, the latter only in minor amounts. Complex **VIII** was previously reported as a major product of a reaction of 'Pd(OAc)$_2$' with 2 equivalents of PPh_3 on heating in methanol (41% yield).[13] It is worth noting that complex **II** is stable in dry THF solutions over 12 hours, which allows for its spectroscopic characterization, but decomposition is seen after ca. 5 days at 22–25 °C.

On changing the Pd/PPh_3 ratio to 1 : 3 complex **II** was not formed, simply a broad resonance at $δ$ 5.71 (FWHM ca. 550 Hz) characterized as $Pd^0(PPh_3)_n$/$[Pd^0(PPh_3)_n(OAc)]P(OAc)PPh_3$ (n = 1, 2 or 3, see Fig. 1(c)). The chemical shift alters with time, with concomitant formation of O=PPh_3, by hydrolysis of $[Ph_3P(OAc)]X$ **IV**, yielding AcOH also. Heating this mixture to 60 °C, over 16 h, eventually ended in decomposition to form large Pd black particles. Indeed, similar ^{31}P NMR spectra were seen on changing the Pd/PPh_3 ratio to 1 : 4, see Fig. 1(d), leading to a mixture of $Pd^0(PPh_3)_3$ **IX** and $[Pd^0(OAc)(PPh_3)_3]^−$ **IX'**. At the same Pd/PPh_3 ratio, subsequent heating to 60 °C resulted in clean conversion of **II** into $Pd^0(PPh_3)_3$ (**IX**), O=PPh_3 (**III**) and 2AcOH, quantitatively, as shown by both ^{31}P and ^1H NMR spectra. Layering this solution with hexane, after t = 16 h, led to the formation of yellow-orange crystals, which were found suitable for X-ray diffraction, establishing the compound as
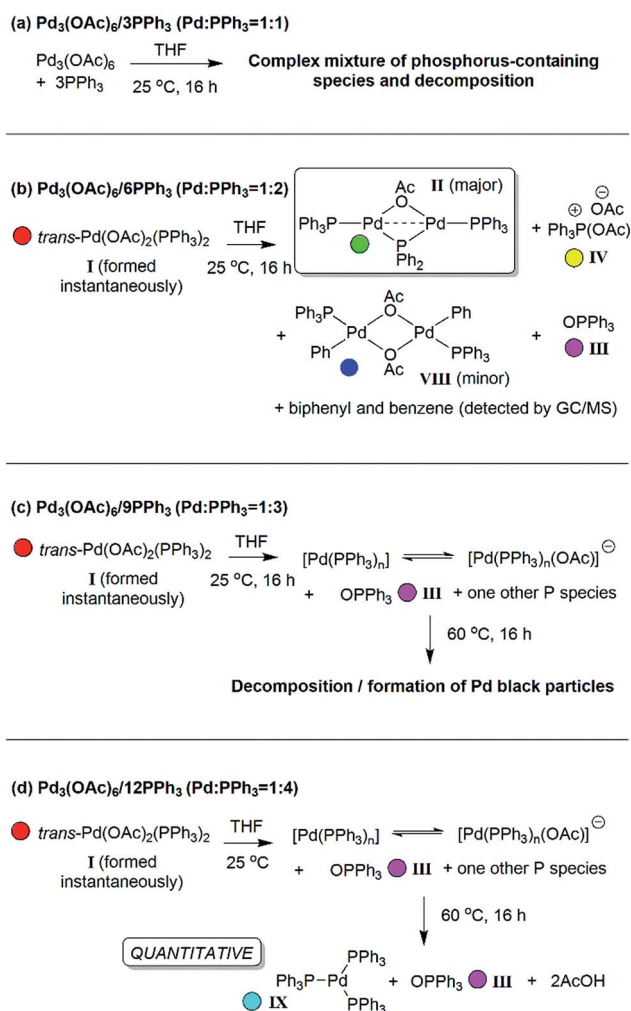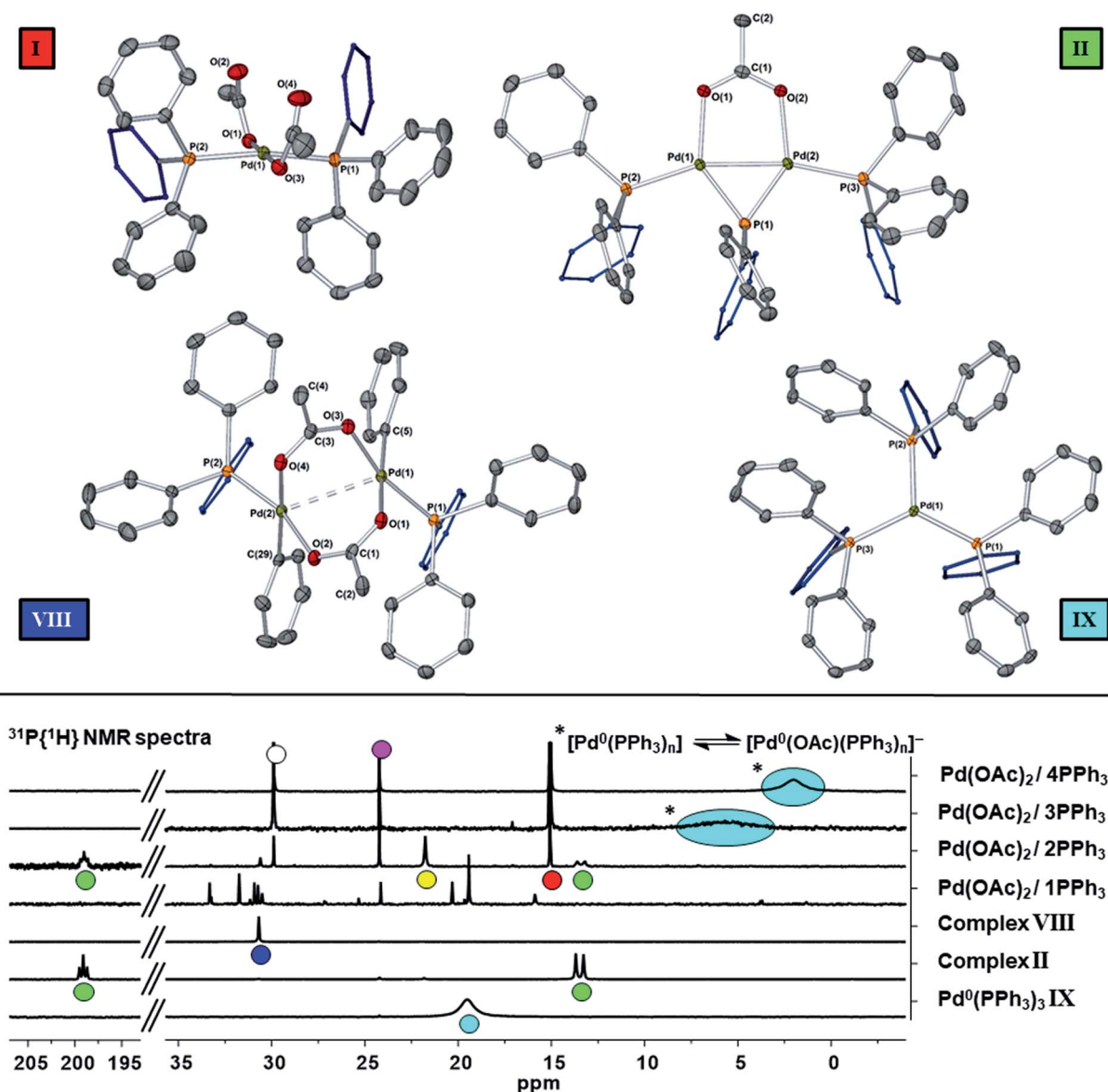
Fig. 2 Top: Single crystal X-ray diffraction structures of **II**, **VIII** and **IX** are shown (thermal ellipsoids shown at 50%, H-atoms and solvent of crystallization not shown, for clarity). Bottom: $^{31}P\{^1H\}$ NMR (202 MHz) spectra of mixtures of 'Pd(OAc)$_2$' with nPPh$_3$ ($n = 1$ to 4) in THF at 23 °C for 16 h, showing differences in phosphorus speciation. Reference spectra are given for **II** (green), **VIII** (blue) and **IX** (cyan); other species are OPPh$_3$ (pink), [AcOPPh$_3$]X (yellow, where X is likely the OAc anion) and *trans*-Pd(OAc)$_2$(PPh$_3$)$_2$ **I** (red). Several phosphorus species are uncharacterized for the Pd(OAc)$_2$/1PPh$_3$ experiment (also resulting in PdNP formation). For the equilibrium shown against the ratio of Pd(OAc)$_2$/4PPh$_3$ spectral data, acetate anion and free PPh$_3$ are involved, explaining the substantially lower chemical shift (compare also the reference spectrum of pure Pd^0(PPh$_3$)$_3$ **IX** – bottom).

Pd^0(PPh$_3$)$_3$ (**IX**) (Fig. 2). It is worthy of note that Pd^0(PPh$_3$)$_3$ **IX** is a relatively stable Pd^0 complex in the solid-state (note: discoloration is noted in air after ~1 day).

Computational studies using DFT calculations with [Pd$_2$(μ-PPh$_2$)(μ$_2$-OAc)(PPh$_3$)$_2$] **II** at the B3LYP/DEF2SVP-D3 level of theory. The calculations reveal a short Pd–Pd bond (2.58 Å), supporting its diamagnetic properties. The HOMO resides primarily on the Pd–Pd centers, whereas the LUMO can be found over the phosphide and Pd–Pd centers (Fig. 3). The HOMO/LUMO provide potential clues about the underlying reactivity of [Pd$_2$(μ-PPh$_2$)(μ$_2$-OAc)(PPh$_3$)$_2$] toward other species such as electrophiles and nucleophiles.

We believe that the mechanism for formation of **II** is different to the Pd^I dimer stabilised by a bridging arene, as reported by Bedford.[10c] In the latter case a sequential reaction in methanol was used, followed by treatment with a non-coordinating anion leaves a suitably-disposed arene to stabilise the cationic Pd^I dimer species, though Pd–π–arene interactions. In **II** acetate takes on that role.

Reactivity of II towards organohalides

The reaction of [Pd$_2$(μ-PPh$_2$)(μ$_2$-OAc)(PPh$_3$)$_2$] **II** with CH$_2$Cl$_2$ **1a** (~10-fold excess) occurred at room temperature to afford a new
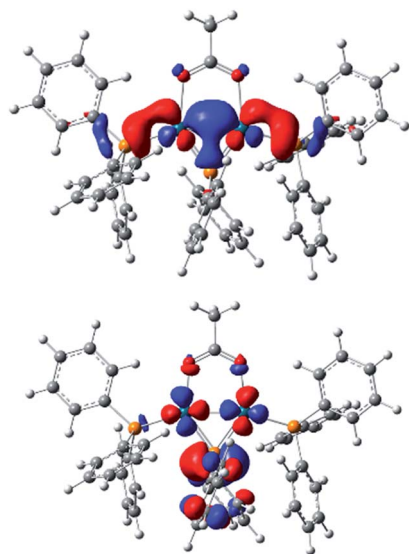
Fig. 3 The HOMO (left) and LUMO (right) for $[Pd_2(\mu\text{-}PPh_2)(\mu_2\text{-}OAc)(PPh_3)_2]$ **II**, computed by density functional theory (b3lyp/def2svp functional/basis set used for optimization, single point orbital and total energies; CPCM implicit solvent (tetrahydrofuran) and Gimme's D3 empirical correction used).

Pd species, which was identified as $[Pd_3(Cl)(PPh_2)_2(PPh_3)_3]OAc$ **Pd₃Cl·OAc** by ESI studies (+ve mode, detected by the $[M - OAc]^+$ ion) (Fig. 4).[14] Real-time reaction monitoring by ^{31}P NMR spectroscopic analysis showed that **Pd₃Cl·OAc** formed over several hours at the expense of **II**. The data for **Pd₃Cl·OAc** closely matches the data obtained from the independent synthesis of $[Pd_3(Cl)(\mu\text{-}PPh_2)_2(PPh_3)_3]Cl$ **Pd₃Cl·Cl**, starting from $PdCl_2(PPh_3)_2$ in aniline under $H_{2(g)}$ at 90 °C, for which an X-ray structure of a single crystal was determined (Fig. 5).[15] We were unable to trace the 'CH₂Cl' fragment derived from CH_2Cl_2, 'Pd(PPh₃)₁' and acetate anion required to balance the overall chemical reaction. However, balance of overall charge and mass allows one to postulate a putative 14-electronic Pd^{II} species **Xa**. Similarly, reaction of **II** with *p*-fluoro-iodobenzene **1b** afforded $[Pd_3(\iota)(\mu\text{-}PPh_2)_2(PPh_3)_4]OAc$ **Pd₃I·OAc**, as shown by ^{31}P NMR and ESI data (as the $[M - OAc]^+$ ion), which degraded rapidly to form Pd black. As with the reaction of **II** with CH_2Cl_2 **1a**, the '*p*-F-C₆H₄-' fragment derived from **1b**, 'Pd(PPh₃)₁' and OAc anion could not be fully traced (Pd^{II} species **Xb** is postulated).

To reveal whether putative 14-electron Pd^{II} species were formed in the reactions of **II** with organohalides (R-X) we hypothesized that a reaction with 2-bromopyridine **1c** would enable characterization by the stabilization conferred by N-coordination from the pyridine ring, leading to formation of a stable 16-electron dinuclear Pd^{II} species (*i.e.* **4a–c**, Fig. 4).

To verify findings concerning formation of $[Pd_3(Br)(\mu\text{-}PPh_2)_2(PPh_3)_3]OAc$ (**Pd₃Br·OAc**) *vide supra*, a closely related sample was prepared by treatment of $[Pd_3(Cl)(\mu\text{-}PPh_2)_2(PPh_3)_3]$ Cl (**Pd₃Cl·Cl**) with excess KBr in CH_2Cl_2, giving $[Pd_3(Br)(\mu\text{-}PPh_2)_2(PPh_3)_3]Br$ (**Pd₃Br·Br**).[16] The latter material possessed identical ^{31}P NMR and MS data to that seen for **Pd₃Br·OAc** from the reaction of **II** with 2-bromopyridine **1c**. A reasonable single

crystal X-ray diffraction structure for **Pd₃Br·Br** was further determined (Fig. 5). Whilst a detailed comparison between **Pd₃Cl·Cl** and **Pd₃Br·Br** cannot be made (R_1 factors for **Pd₃Cl·Cl** = 3.58% and **Pd₃Br·Br** = 7.04%), there are striking structural differences that necessitate additional comment. The cyclic 6-membered 'Pd–P–Pd–Cl–Pd–P' fragment is essentially flat in **Pd₃Cl·Cl**, leaving the second chloride anion as non-coordinating. However, in **Pd₃Br·Br** we see something quite different – the cyclic 6-membered 'Pd–P–Pd–Br–Pd–P' fragment is highly twisted, which is associated with an interacting second bromide anion.

It is tempting to draw an analogy here to a bromonium ion interacting with a bromide anion (*i.e.* reactions of alkenes with bromide proceeding *via* bromonium ion intermediates). The structural differences between **Pd₃Cl·Cl** and **Pd₃Br·Br** suggest that they could be distinctly different in how they operate in catalysis.

The relevance of our findings concerning reaction of **II** with organohalides requires contextualisation with the results recently reported by Schoenebeck and co-workers.[17] It has been shown that $[Pd(\mu\text{-}I)P(t\text{-}Bu)_3]_2$ reacts with $PHPh_2$ (slight excess relative to the Pd^I dimer) in toluene at room temperature to give a Pd_3 cluster containing three bridging phosphide ligands (Fig. 6). Subsequent reaction with an aryl halide then delivers a Pd_3-type cluster containing a bridging iodide ligand, similar to the **Pd₃X·X** clusters *vide supra*. The pathways to these Pd_3 clusters are not the same. Complex **II** reacts directly with organohalides to give **Pd₃X·X** clusters (where X = Cl, Br or I), *i.e.* additional phosphine is not necessary at this point. Indeed, if additional PPh_3 (2 equiv.) is reacted with **II** (1 equiv.) in THF at room temperature we see the generation of $Pd(PPh_3)_n$ species (where $n = 3$, this species was detected by LIFDI-MS, see ESI†). This finding is in-keeping with what was observed when $Pd_3(OAc)_6$ was reacted with nine equivalents of PPh_3 (*i.e.* Pd/PPh_3 ratio of 1 : 3, Fig. 2). We expect that Pd^0 complexes are generated from disproportionation of the Pd^I dinuclear complex **II**, upon addition of PR_3, akin to the observations reported by Schoenebeck and Colacot.[10b]

Importance of our findings in an exemplar SMCC reaction

To better understand the importance of the 'Pd(OAc)₂'/nPPh₃ ratio in catalysis, the cross-coupling of 2-bromopyridine **1c** with *p*-fluorophenylboronic acid **2** to give 2-arylpyridine **3** was examined,[6b] using 1 M n-Bu₄NOH as the base, in a THF/water mixture (1 : 1, v/v) at 40 °C. We carefully selected 1 M n-Bu₄NOH as the base, drawing on the recent findings concerning the importance of both the hydroxide anion and cation-type in SMCCs.[18] Also pertinent to mention is that our SMCC reaction is homogeneous, *i.e.* not biphasic, simplifying the discussion concerning which phase the Pd catalyst and organoboron species reside in. Furthermore, operationally NMR spectroscopic analysis *in operando* was made feasible by use of aqueous n-Bu₄NOH in THF.

SMCC reactions of **1c** + **2** → **3** were monitored *in operando* by ^{1}H NMR spectroscopic analysis, allowing pre-stirred mixtures of 'Pd₃(OAc)₆'/nPPh₃ (n = 6 and 12, *i.e.* Pd/PPh₃ = 1 : 2 or 1 : 4
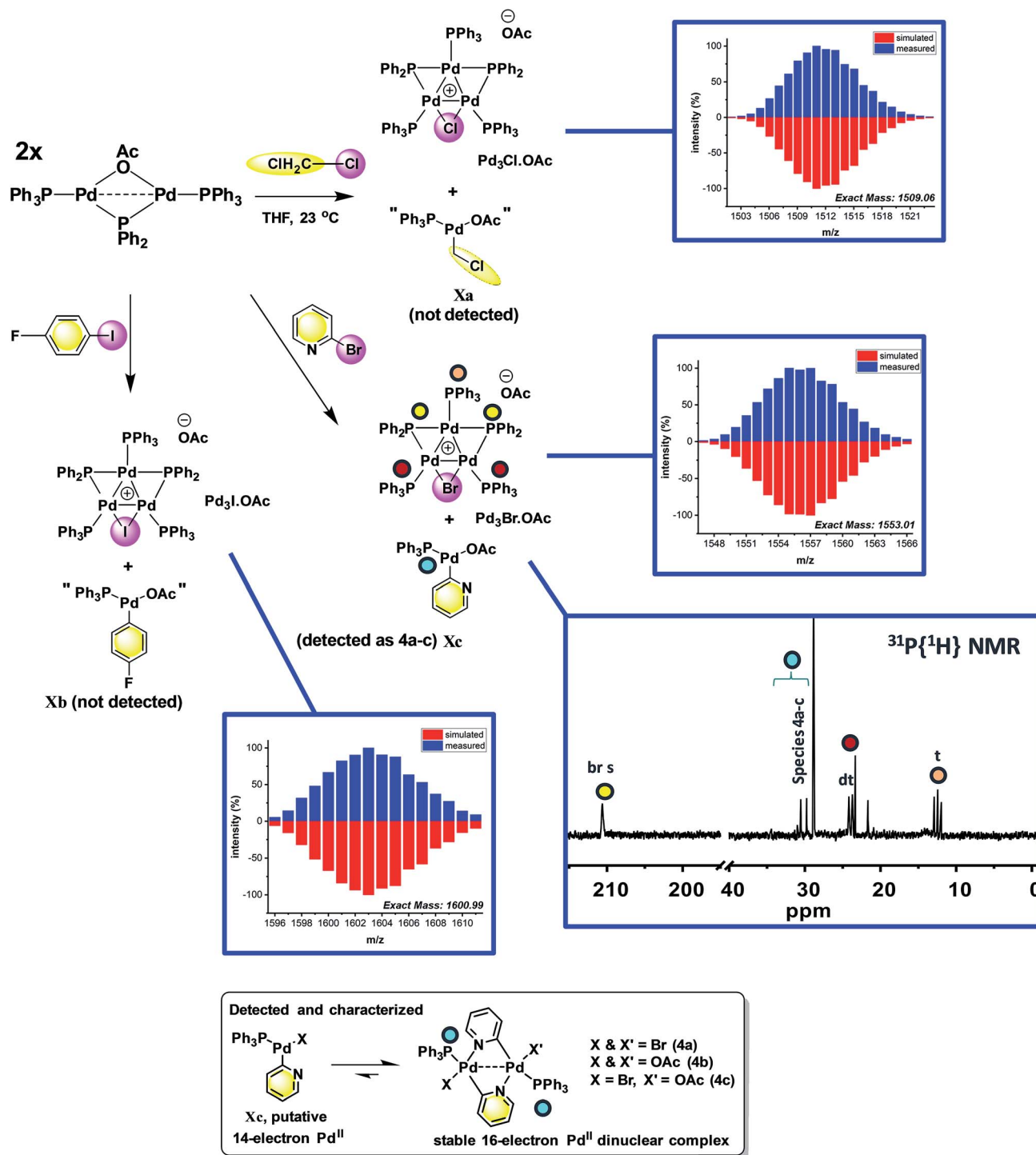
Fig. 4 Reactions of dinuclear PdI complex **II** with organohalides (**1a–c**), leading to formation of Pd$_3$ clusters **Pd$_3$X·OAc**. The X anions in these clusters are likely acetate (mass balance is formally correct using acetate for all Pd species formed), although mixtures of different anions cannot be ruled out for species generated *in situ*. The MS ions are all observed by ESI (+ve mode) as molecular cations, the data for which is presented (measured – in blue; simulated – in red). The ^{31}P{^{1}H} NMR spectrum for species generated from the reaction of 2-bromopyridine **1c** with **II** illustrates the formation of **Pd$_3$Br·OAc** and species **4a–c** (note a cut//in the ^{31}P NMR spectrum is made between 40 and 190 ppm, due to the wide spectral range, for ease of viewing – full ^{31}P NMR spectra are shown in the ESI†).

respectively) to be compared in THF against a reaction mediated by [Pd$_2$(μ-PPh$_2$)(μ$_2$-OAc)(PPh$_3$)$_2$] **II**. The kinetic profiles for the appearance of **3**, with concomitant disappearance of **1c**

(pseudo-zero order in **1c**), are shown in Fig. 6. The kinetic profile for the reaction mediated by Pd$_3$(OAc)$_6$/6PPh$_3$ (1 : 2, Pd/PPh$_3$) indicates that the reaction is efficient at 40 °C {Fig. 7(A)} –
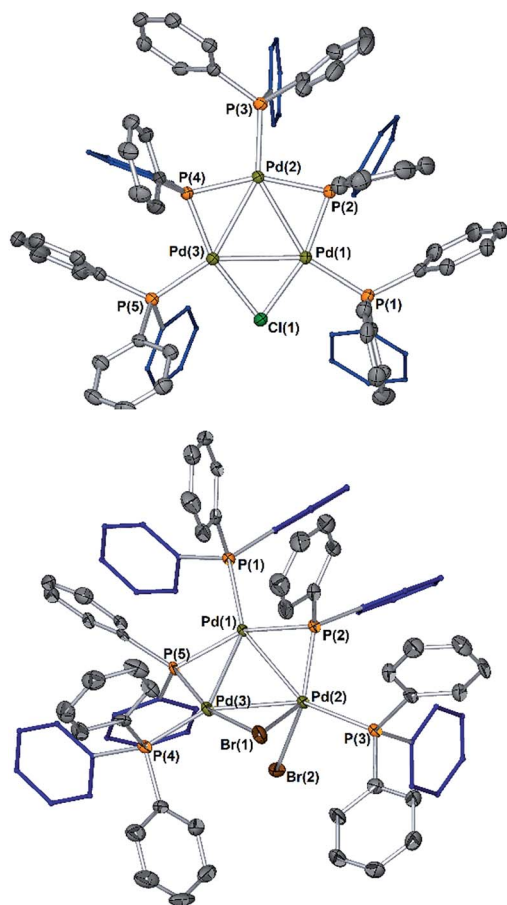
Fig. 5 The single crystal X-ray diffraction structures for [Pd₃(-X)(PPh₂)₂(PPh₃)₃]X (top, X = Cl, **Pd₃Cl·Cl**; bottom, X = Br, **Pd₃Br·Br**); H-atoms and solvent of crystallization are not shown and thermal ellipsoids are set at 50% probability. For **Pd₃Cl·Cl** the non-coordinating chloride anion is not shown. Selected bond lengths (Å) and angles (°) for: **Pd₃Cl·Cl** Cl1–Pd1 = 2.3828(8); Cl1–Pd3 = 2.4002(8); Pd1–Pd2 = 2.9138(3); Pd1–Pd3 = 2.8882(3); Pd2–Pd3 = 2.9127(3); Pd1–Cl1–Pd3 = 74.29(2); Pd1–P2–Pd2 = 81.38(3); Pd3–P4–Pd2 = 81.45(3); Cl1–Pd1–Pd2 = 113.303(19); Cl1–Pd1–Pd3 = 53.130(18); Pd3–Pd1–Pd2 = 60.265(8). **Pd₃Br·Br** Pd1–Pd2 = 2.8355(10); Pd2–Br1 = 2.9423(13); Pd2–Br2 = 2.5698(13); Pd3–Br1 = 2.5490(13); Pd1–Pd3 = 2.8808(10); Pd2–Pd3 = 2.8240(10); Pd2–Pd1–Pd3 = 59.21(2), Pd3–Pd2–Pd1 = 61.20(2), Pd2–Pd3–Pd1 = 59.60(2); Pd3–Br1–Pd2 = 61.40(3); Br2–Pd2–Pd1 = 101.20(4); Br2–Pd2–Pd3 = 76.91(3); Br2–Pd2–Br1 = 96.67(4).

there is an exotherm during initial catalyst turnover (ca. 4 turnovers) which is associated with full dissolution of aqueous 1 M n-Bu₄NOH (into THF – overall concentration equals 0.5 M n-Bu₄NOH). The same reaction mediated by **II** showed a similar kinetic curve {Fig. 7(B)}, confirming the catalytic competency of this key species isolated earlier. Furthermore, no Pd particles were visibly seen to form during catalysis (the solution appearing completely homogeneous).

Altering the Pd₃(OAc)₆/12PPh₃ (1 : 4, Pd/PPh₃) led to a poor catalyst system for reaction **1c + 2 → 3** at 40 °C {Fig. 7(C), curves illustrated by diamonds}. This catalyst system exhibited higher catalyst efficacy at 70 °C. Thus, additional phosphine slows down catalysis in the reaction of **1c + 2 → 3**, at 40 °C, which is
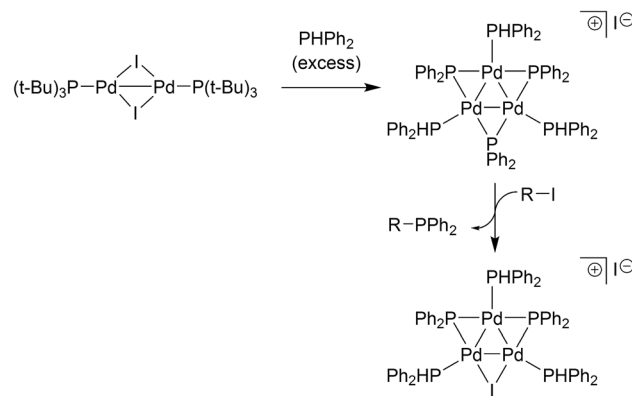

Fig. 6 Schoenebeck's findings[17] on the formation of a Pd₃-type cluster from an electron-rich Pdᴵ dimer species.

an outcome consistent with our previous studies on SMCCs involving **1c**.[6b]

With the finding that [Pd₂(μ-PPh₂)(μ₂-OAc)(PPh₃)₂] **II** reacts with 2-bromopyridine **1c** to give [Pd₃(Br)(μ-PPh₂)₂(PPh₃)₃]OAc (**Pd₃Br·OAc**) and [Pd(X/X′)(N,C²-pyr)(PPh₃)]₂ (**4a–c**), additional catalytic experiments were devised to test the importance of such species in the SMCC reaction **1c + 2 → 3** (Fig. 8). Two control experiments, with different Pd catalysts, were conducted: (a) to establish the catalytic competency of **Pd₃Br·Br**;[19] (b) to assess the catalytic activity of [Pd(Br)(N,C²-pyr)(PPh₃)]₂ **4a**, under comparable reaction conditions. The reaction of **1c + 2 →**
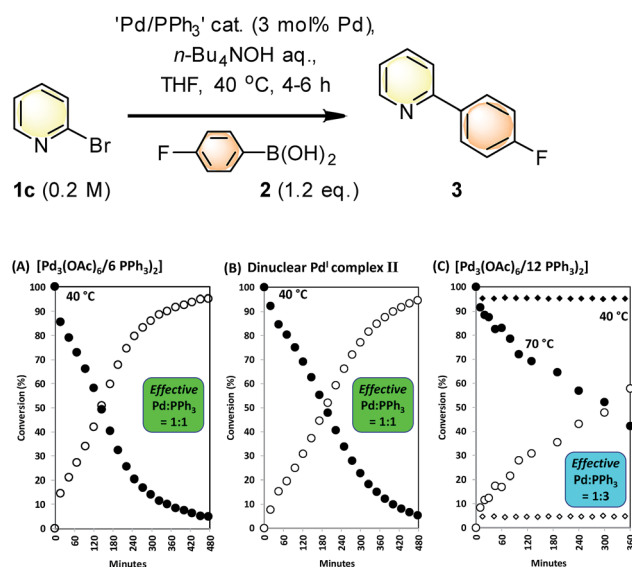
Fig. 7 Kinetic profiles for the SMCC reaction of **1c + 2** to give **3**, mediated by Pd(OAc)₂/nPPh₃ (n = 2 and 4) and dinuclear Pdᴵ complex **II**. (A) Reaction mediated by Pd₃(OAc)₆/6PPh₃; (B) reaction mediated by dinuclear Pdᴵ complex **II**; (C) reaction mediated by Pd₃(OAc)₆/12PPh₃. Reactions were monitored by ¹H NMR spectroscopic analysis in a J. Young's NMR tube (spinning). The effective Pd : PPh₃ ratio takes into account that one equivalent of PPh₃ is required to reduce Pdᴵᴵ to Pd⁰, with concomitant formation of one equivalent of O=PPh₃. For complex **II**, two PPh₃ ligands are present overall, i.e. one per Pd; in this respect the 'PPh₂' group was treated as an anionic ligand.

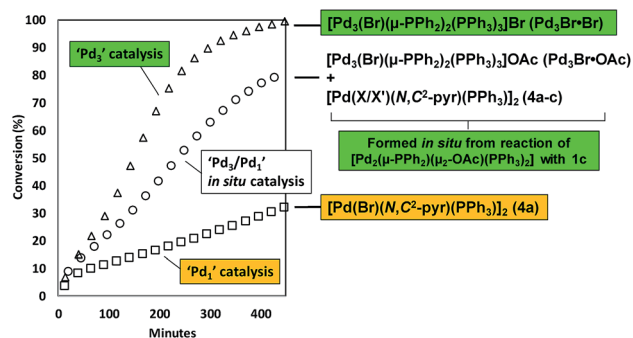**Fig. 8** Overlay of kinetic curves for the SMCC reaction of **1c** + **2** → **3**, mediated by **Pd₃Br·Br** (1 mol%), **4a** (0.5 mol%) and **II** (1.5 mol%, generating **Pd₃Br·OAc**, **4a–c** in situ); other reaction conditions identical to Fig. 6. Reactions were monitored by ^{1}H NMR spectroscopic analysis in a J. Young's NMR tube (spinning).

3, mediated by **Pd₃Br·Br** (1 mol%, giving 1 mol% active Pd – the cluster being treated as a well-defined catalyst species[11]) gave **3** with full conversion after *ca.* 7.5 h at 40 °C (Fig. 8). The same reaction mediated by an authentic sample of **4a** (0.5 mol% giving 1 mol% active Pd[6b]) gave **3** with 32% conversion after *ca.* 7.5 h. These control experiments establish that **Pd₃Br·Br** is a significantly more active catalysis species than **4a**. Thus, when generated *in situ*, we expect **Pd₃Br⁺** species to play a more dominant role in terms of the overall catalyst efficacy *vide infra*.

With the kinetic profiles for the SMCC reaction of **1c** + **2** → **3**, mediated by either **Pd₃Br·Br** or **4a**, established, we could then qualitatively compare the catalytic activity mediated by **Pd₃-Br·OAc** and $[Pd(X/X')(N,C^2\text{-pyr})(PPh_3)]_2$ (**4a–c**) species, formed *in situ* from the reaction of **II** with **1c**.[20] The observed catalyst activity sits between the high reactivity of **Pd₃Br·Br** and comparatively lower activity of $[Pd(Br)(N,C^2\text{-pyr})(PPh_3)]_2$ **4a**.

Conclusion

In conclusion we have demonstrated that reaction of $Pd_3(OAc)_6$ with 6 equivalents of PPh_3, that is in a Pd/PPh_3 ratio of 1 : 2, gives an intriguing dinuclear Pd^I complex, $[Pd_2(\mu\text{-}PPh_2)(\mu_2\text{-}OAc)(PPh_3)_2]$, **II**. Species **II** is relatively unstable, but characterizable, and we propose it is this species that Amatore and Jutand detected in their early studies, which resisted characterization at that time.[4a] An important discovery was the finding that **II** reacts relatively cleanly with the organohalides, CH_2Cl_2 (**1a**), *p*-fluoroiodobenzene (**1b**) and 2-bromopyridine (**1c**) to afford Pd₃ cluster complexes containing bridging halide ligands, *i.e.* $[Pd_3(X)(PPh_2)_2(PPh_3)_3]X$, carrying an overall 4/3 oxidation state. Use of 2-bromopyridine **1c** was critical in understanding that a putative 14-electron mononuclear '$Pd^{II}(R)(X)(PPh_3)$' is released on forming $[Pd_3(X)(PPh_2)_2(PPh_3)_3]X$ clusters from **II**. Altering the Pd/PPh_3 ratio from 1 : 2 to 1 : 4 forms $Pd^0(PPh_3)_3$ quantitatively, generally in-keeping with Amatore's and Jutand's original studies.[4] It has been established further that the Pd/PPh₃ ratios are important in an exemplar SMCC reaction, Pd/PPh₃ ratio Pd/PPh_3 reaction, **1c** + **2** → **3**. Near identical catalytic efficacy was seen for a reaction mediated by either $1Pd(OAc)_2$/

$2PPh_3$ or **II**, whereas the $1Pd(OAc)_2/4PPh_3$ catalyst system was significantly less effective, requiring a higher temperature (70 rather than 40 °C) for reasonable conversion to product **3** to be observed.

An important take home message from our study is that where $[Pd_2(\mu\text{-}PPh_2)(\mu_2\text{-}OAc)(PPh_3)_2]$ **II** can form, *i.e.* when a ratio of Pd/PPh_3 ratio is 1 : 2 employed in catalysis, reactions with organohalides (common starting materials for cross-coupling catalysis) afford catalytically competent Pd₃ cluster complexes *in situ*, in addition to other known Pd^{II} species (*i.e.* oxidative addition products). If the relative amount of PPh₃ ligand to Pd is low, then Pd clustering tends to occur, to afford either particles (where $Pd/PPh_3 = 1 : 1$), or 'ligated clusters', whereas well-defined dimers and trimers are formed where $Pd/PPh_3 = 1 : 2$ (the major finding of this study) and when there is enough PPh₃ ligand around, mono-nuclear $Pd^0(PPh_3)_n$, *i.e.* $n > 2$, can be stabilised, aligning with a general understanding of ligated Pd^0 species in text book mechanisms.

Understanding how $[Pd_3(X)(\mu\text{-}PPh_2)_2(PPh_3)_3]X$ clusters activate aryl/heteroaryl halides and organometallic coupling partners, *e.g.* aryl boronic acids,[11] will no doubt be important going-forwards, which will enable their catalytic properties to be fully delineated and exploited in chemical synthesis. To emphasize this point further, similar Pd₃-type clusters have been studied by Maestri and Malacria in catalysis, particularly hydrogenation.[21] Our results, taken together with contributions made by others, show that Pd₃-clusters are ripe for exploitation in applied catalysis.

Conflicts of interest

There are no conflicts to declare.

Acknowledgements

Notes and references

1 (a) K. C. Nicolaou, P. G. Bulger and D. Sarlah, *Angew. Chem., Int. Ed.*, 2005, **44**, 4442–4489; (b) C. Torborg and M. Beller, *Adv. Synth. Catal.*, 2009, **351**, 3027–3043; (c) W. A. Carole and T. J. Colacot, *Chem.–Eur. J.*, 2016, **22**, 7686–7695; (d) I. J. S. Fairlamb, *Angew. Chem., Int. Ed.*, 2015, **54**, 10415–10427; (e) P. Devendar, R.-Y. Qu, W.-M. Kang, B. He and G.-F. Yang, *J. Agric. Food Chem.*, 2018, **66**, 8914–8934.

2 (a) T. A. Stromnova, V. S. Sergienko, A. V. Kisin, M. A. Porai-Koshits and I. I. Moiseev, *Bull. Acad. Sci. USSR, Div. Chem. Sci.*, 1987, **36**, 821–824; (b) V. S. Sergienko and M. A. Porai-Koshits, *J. Struct. Chem.*, 1988, **28**, 548–552.

3 J. A. Labinger, *Organometallics*, 2015, **34**, 4784–4795.

4 In the original publication it was shown that *trans*-Pd(OAc)$_2$(PPh$_3$)$_2$ forms an unstable Pd(0) species – excess PPh$_3$ was required to form oxidative addition products of the type *trans*-Pd(I)Ph(PPh$_3$)$_2$ by reaction of Pd(PPh$_3$)$_2$ with PhI, see: (*a*) C. Amatore, A. Jutand and M. A. M'Barki, *Organometallics*, 1992, **11**, 3009–3013. The subsequent study employed higher PPh$_3$/Pd(OAc)$_2$ ratios, see: (*b*) C. Amatore, E. Carre, A. Jutand and M. A. M'Barki, *Organometallics*, 1995, **14**, 1818–1826. For the reactions of acetate anion with Pd(PPh$_3$)$_4$, see: (*c*) C. Amatore, E. Carre, A. Jutand, M. A. M'Barki and G. Meyer, *Organometallics*, 1995, **14**, 5605–5614. The global findings by Amatore and Jutand led to the proposal of anionic Pd intermediates playing a critical role in cross-coupling catalysis, see: (*d*) C. Amatore and A. Jutand, *Acc. Chem. Res.*, 2000, **33**, 314–321.

5 The reaction of Pd(OAc)$_2$ with 2PPh$_3$ was reported, leading to the proposal that a Pd^0(PPh$_3$)$_n$ species was formed, see: Z. Csákai, R. Skoda-Földes and L. Kollár, *Inorg. Chim. Acta*, 1999, **286**, 93–97.

6 The Pd/L ratio is important for effective cross-coupling catalysis, see: (*a*) U. Christmann and R. Vilar, *Angew. Chem., Int. Ed.*, 2005, **44**, 366–374. The effect of the Pd/PPh$_3$ was also previously examined by us, see: (*b*) Suzuki–Miyaura cross-couplings, see: A. Beeby, S. Bettington, I. J. S. Fairlamb, A. E. Goeta, A. R. Kapdi, E. H. Niemela and A. L. A. Thompson, *New J. Chem.*, 2004, **28**, 600–605. A ratio of Pd(OAc)$_2$/PAr$_3$ of 1 : 2 was found optimal for SMCC reactions involving purines, see: (*c*) T. E. Storr, J. A. Strohmeier, C. G. Baumann and I. J. S. Fairlamb, *Chem. Commun.*, 2010, **46**, 6470–6472.

7 D. Perera, J. W. Tucker, S. Brahmbhatt, C. J. Helal, A. Chong, W. Farrell, P. Richardson and N. W. Sachs, *Science*, 2018, **359**, 429–434.

8 J. M. Granda, L. Donina, V. Dragone, D.-L. Long and L. Cronin, *Nature*, 2018, **559**, 377–381.

9 (*a*) S. V. Ley, D. E. Fitzpatrick, R. J. Ingham and R. M. Myers, *Angew. Chem., Int. Ed.*, 2015, **54**, 3449–3464; (*b*) M. Trobe and M. D. Burke, *Angew. Chem., Int. Ed.*, 2018, **57**, 4192–4214.

10 (*a*) D. P. Hruszkewycz, D. Balcells, L. M. Guard, N. Hazari and M. Tilset, *J. Am. Chem. Soc.*, 2014, **136**, 7300–7316; (*b*) C. C. C. Johansson Seechurn, T. Sperger, T. G. Scrase, F. Schoenebeck and T. J. Colacot, *J. Am. Chem. Soc.*, 2017, **139**, 5194–5200; (*c*) M. Montgomery, H. M. O'Brien, C. Méndez-Gálvez, C. R. Bromfield, J. P. M. Roberts, A. M. Winnicka, A. Horner, D. Elorriaga, H. A. Sparkes and R. B. Bedford, *Dalton Trans.*, 2019, **48**, 3539–3542; (*d*) S. Wagschal, L. A. Perego, A. Simon, A. Franco-Espejo, C. Tocqueville, J. Albaneze-Walker, A. Jutand and L. Grimaud, *Chem.–Eur. J.*, 2019, **25**, 6980–6987.

11 The catalytic competency of the Pd$_3$ cluster has been validated in Suzuki–Miyaura cross-couplings, see: F. Fu, J. Xiang, H. Cheng, L. Cheng, H. Chong, S. Wang, P. Li, S. Wei, M. Zhu and Y. Li, *ACS Catal.*, 2017, **7**, 1860–1867.

12 (*a*) D. P. Hruszkewycz, J. Wu, N. Hazari and C. D. Incarvito, *J. Am. Chem. Soc.*, 2011, **133**, 3280–3283; (*b*) P. Leoni, E. Vichi, S. Lencioni, M. Pasquali, E. Chiarentin and A. Albinati, *Organometallics*, 2000, **19**, 3062–3068.

13 The reaction of Pd(OAc)$_2$/2PPh$_3$ in MeOH gives complex **VIII** in 41% yield, see. M. B. Hursthouse, O. D. Sloan, P. Thornton and N. P. C. Walker, *Polyhedron*, 1986, **5**, 1475–1478.

14 In [Pd$_3$(Cl)(PPh$_2$)$_2$(PPh$_3$)$_3$]OAc we specify the non-coordinating anion as acetate, which serves to balance the full chemical reaction equation. As the reaction is run with an excess of CH$_2$Cl$_2$, exchange of acetate for chloride could occur under the reaction conditions used.

15 A. S. Berenblyum, A. P. Aseeva, L. I. Lakhman and I. I. Moiseev, *J. Organomet. Chem.*, 1982, **234**, 219–235.

16 K. R. Dixon and A. D. Rattray, *Inorg. Chem.*, 1978, **17**, 1099–1103.

17 C. J. Diehl, T. Scattolin, U. Englert and F. Schoenebeck, *Angew. Chem., Int. Ed.*, 2019, **58**, 211–215.

18 (*a*) K. Matos and J. A. Soderquist, *J. Org. Chem.*, 1998, **63**, 461–470; (*b*) A. F. Schmidt, A. A. Kurokhtina and E. V. Larina, *Russ. J. Gen. Chem.*, 2011, **81**, 1573–1574; (*c*) B. P. Carrow and J. F. Hartwig, *J. Am. Chem. Soc.*, 2011, **133**, 2116–2119; (*d*) C. Amatore, A. Jutand and G. Le Duc, *Chem.–Eur. J.*, 2011, **17**, 2492–2503; (*e*) C. Amatore, A. Jutand and G. Le Duc, *Chem.–Eur. J.*, 2012, **18**, 6616–6625; (*f*) A. J. J. Lennox and G. C. Lloyd-Jones, *Angew. Chem., Int. Ed.*, 2013, **52**, 7362–7370; (*g*) A. A. Thomas, H. Wang, A. F. Zahrt and S. E. Denmark, *J. Am. Chem. Soc.*, 2017, **139**, 3805–3821.

19 **Pd$_3$Br·Br** was selected for control experiments as we hypothesized that excess bromide would be generated the SMCC reaction, *i.e.* bromide would be liberated during each catalyst turnover.

20 A catalyst loading approximation (1.5 mol% of **II**) was made for comparison of catalytic activity for the *in situ* generation of **Pd$_3$Br·OAc** and **4a**, which takes into consideration that degradation of **II** is expected under the real working reaction conditions.

21 (*a*) S. Blanchard, L. Fensterbank, G. Gontard, E. Lacte, G. Maestri and M. Malacria, *Angew. Chem., Int. Ed.*, 2014, **53**, 1987–1991; (*b*) A. Monfredini, V. Santacroce, P.-A. Deyris, R. Maggi, F. Bigi, G. Maestri and M. Malacria, *Dalton Trans.*, 2016, **45**, 15786–15790; (*c*) A. Monfredini, V. Santacroce, L. Marchio, R. Maggi, F. Bigi, G. Maestri and M. Malacria, *ACS Sustainable Chem. Eng.*, 2017, **5**, 8205–8212.